ELSEVIER

Physica D 77 (1994) 456–472

PHYSICA D

Information cascade with marginal stability in a network of chaotic elements

Kunihiko Kaneko

Department of Pure and Applied Sciences, College of Arts and Sciences, University of Tokyo, Komaba, Meguro-ku, Tokyo 153, Japan

Received 6 January 1994; accepted 31 March 1994
Communicated by Y. Kuramoto

Abstract

A newly discovered cascade process of clusters is studied in a network of chaotic elements. It is shown that the splitting of clusters and the synchronization of elements are balanced in a class of partially ordered states, where marginal stability is sustained over an interval of the bifurcation parameters. The partition information creation in bit space shows an avalanche process of information, which leads to the anomalous behavior of power spectra, roughly fitted by a power law form of the wavenumber. Lyapunov spectra have accumulation at null exponents, analogous with those studied in fluid turbulence models.

1. Introduction

Globally coupled dynamical systems have been a focus of interest [1–7] in a broad range of fields, including neurodynamics, fluid dynamics, condensed matter physics such as Josephson junction arrays and charge density waves, optics, evolution dynamics, and economics. "Globally coupled map" (GCM) [1,4] can provide a standard model for universal behavior in these systems. The simplest model for the GCM is given by

$$x_{n+1}(i) = (1-\epsilon)f(x_n(i)) + \frac{\epsilon}{N}\sum_{j=1}^{N} f(x_n(j)), \tag{1}$$

where n is a discrete time step and i is the index for elements ($i = 1, 2, \ldots, N$ = system size). Here we choose the logistic map $f(x) = 1 - ax^2$ as the local element in Eq. (1), to obtain the simplest model for globally coupled chaotic systems.

An important notion in globally coupled dynamical systems is *clustering*. After our system falls on an attractor, elements $x_n(i)$ split into clusters. Here, elements belonging to the same cluster L take exactly identical values X_n^L. This variable X_n^L can change in time, but the clustering condition itself is invariant after our system falls on an attractor. Clustering is characterized by the number of

0167-2789/94/$07.00
SSDI 0167-2789(94)00110-C

clusters k and the number of elements in each cluster, given by $[N_1, N_2, \ldots, N_k]$ ($\sum_{j=1}^{k} N_j = N$) (for details see [4]). According to the clustering distribution for an attractor, four phases are known to exist in globally coupled dynamical systems; (i) coherent phase, where only a single synchronized attractor ($k = 1$) exists; (ii) ordered phase, where attractors have small numbers of clusters ($k \ll N$); (iii) partially ordered (PO) phase; where a variety of clusterings coexist; some have a large number of clusters, while others have few; (iv) turbulent phase, where all elements are completely desynchronized ($k = N$).

As is discussed in [4], the model (1) has two tendencies, synchronization by the mean field averaging and desynchronization by the chaotic instability. If the former tendency wins, the system falls on a coherent state, while it is attracted to a turbulent state if the latter wins [4].

In the PO phase, these two tendencies are somewhat balanced. Here we study this phase in more detail. As is shown in the phase diagram in [4], there are two distinct PO phases; one between the coherent and ordered phases (for $\epsilon > 0.2$ and $a > 1.5$), and the other between the ordered and turbulent phases. The latter PO phase (type I) has been studied with an emphasis on the chaotic itinerancy there, while the former PO phase (type II) has not been explored well yet. In the present paper, we show that the partially ordered phase of type II satisfies the marginal stability condition. We will also elucidate that there is a cascade process of clusters in bit space, as is characterized by the flow of partition information. This cascade process is quite analogous to the one in fluid turbulence.

The paper is organized as follows. In Section 2, the marginal stability of the partially ordered phase is shown, and the splitting exponent is introduced. The cascade process of clusters is demonstrated in Section 3, with the help of partition information creation. An information avalanche in bit space is displayed. To pursue the analogy with the cascade process of vortices in turbulence, we compute power spectra and Lyapunov spectra in Section 4. Section 5 is devoted to discussions and a summary.

2. Marginal stability

We first introduce a characteristic exponent which enables us to measure the degree of synchronization in a network. First we note that the distance between the values of two elements $x_n(j)$ and $x_n(j) = x_n(i) + \delta$ is amplified or reduced by

$$x_{n+1}(j) - x_{n+1}(i) = (1 - \epsilon) f'(x_n(i))\, \delta, \tag{2}$$

for small δ. Thus the criterion of splitting between an element i and another element whose value is close to $x_n(i)$, is given by the exponent

$$\lambda_{\mathrm{spl}}(i) = \lim_{T \to \infty} \frac{1}{T} \sum_{n}^{T} \log |(1 - \epsilon) f'(x_n(i))|. \tag{3}$$

We note that this splitting exponent $\lambda_{\mathrm{spl}}(i)$ is different from the Lyapunov exponent, which gives the amplification rate of a tiny difference of two orbits in phase space, while our splitting exponent gives the rate of the amplification of a tiny difference between two elements for a single orbit.

If two elements belong to the same synchronized cluster, the exponent $\lambda_{\mathrm{spl}}(i)$ should be negative, otherwise the clusters would split at some time. For an element which is not a part of clusters, it

is found that $\lambda_{\rm spl}(i)$ is positive. For example, all of the splitting exponents $\lambda_{\rm spl}(i)$ are positive in the turbulent phase. At the partially orderered phase (type II), the exponents are positive for the elements with $N_j = 1$ and negative for those with $N_j > 1$.

For the characterization of the temporal change of clustering, it is useful to introduce a "local" splitting exponent, averaged over only a given finite number of time steps T,

$$\lambda^T_{\rm spl}(i,n) = \frac{1}{T}\sum_{m=n}^{n+T} \log|(1-\epsilon)f'(x_m(i))|. \tag{4}$$

In the partially ordered phase, the exponents often fluctuate around 0, but they can also remain negative over long periods of time, while the corresponding elements tend to be synchronized. Such a long time maintenance of negative values often leads to a reduction of the difference of two elements down to the minimal bit in our digital computer. Indeed, in the PO phase, we have found that this reduction lasts over so long time steps that it often proceeds to the minimum bit through the course of a very long time simulation. Once the difference between two elements is reduced to the minimal bit, it remains zero in a digital computer, even if $\lambda^T_{\rm spl}(i,n)$ becomes positive again and the coherence turns out to be unstable.

In Fig. 1, we have plotted a time series of $\lambda^T_{\rm spl}(i,n)$. Up to the time steps indicated by the arrow, the system is in a few-cluster state, but some of the exponents $\lambda^T_{\rm spl}(i,n)$ are slightly positive for elements in clusters with $N_i > 1$. Thus this state should be unstable when computations with infinite precision are performed.

Hence it is hard to simulate the model (1) correctly in our digital computer. In order to remove such numerical errors, we introduce a tiny noise term to Eq. (1), which at the same time also takes into account of the noise inherent to natural systems. Thus the model we study here is given by

$$x_{n+1}(i) = (1-\epsilon)f(x_n(i)) + \frac{\epsilon}{N}\sum_{j=1}^{N} f(x_n(j)) + \sigma_n(i), \tag{5}$$

where the noise term $\sigma_n(i)$ is homogeneously distributed over $[-\delta,\delta]$. In Fig. 1, we have added noise with $\sigma = 10^{-8}$ at the time step indicated with the arrow. With this addition of noise, the system steps out from the digitalization-induced pseudo-attractor. In Fig. 1a (corresponding to type II PO), the system goes to a state with marginal stability, to be discussed later. In Fig. 1b (type-I PO), the system is attracted to a 4-cluster state ($N_1 = 21, N_2 = 18, N_3 = 8, N_4 = 3$), which is a real attractor. Indeed all of the splitting exponents $\lambda_{\rm spl}(i)$ are negative, while those for the third and fourth cluster are slightly positive for the pseudo-attractor state (with $N_1 = 21, N_2 = 16, N_3 = 7, N_4 = 6$) found without the noise term. Throughout the latter part of the present paper, the noise term is applied at all time steps.

Let us now focus on the type-II PO phase, where no few-cluster attractor could be detected, when noise is applied. The distribution of the exponent $\lambda^T_{\rm spl}(i,n)$ (for $T = 128$) is given in Fig. 2, sampled over all elements and many time steps. The distribution has a sharp peak near zero, implying that the stability for synchronization is marginal. Hence the splitting of clusters and synchronization of elements are balanced. The two processes are temporally separated as distinct regimes. Over long periods of time, the elements may almost completely be synchronized, till amplification of tiny differences dominates.

Due to the balance between synchronization of elements and splitting of clusters, the average value of $\lambda_{\rm spl}(i)$ is close to zero. In Fig. 3, the exponent is plotted versus a. We can clearly see that

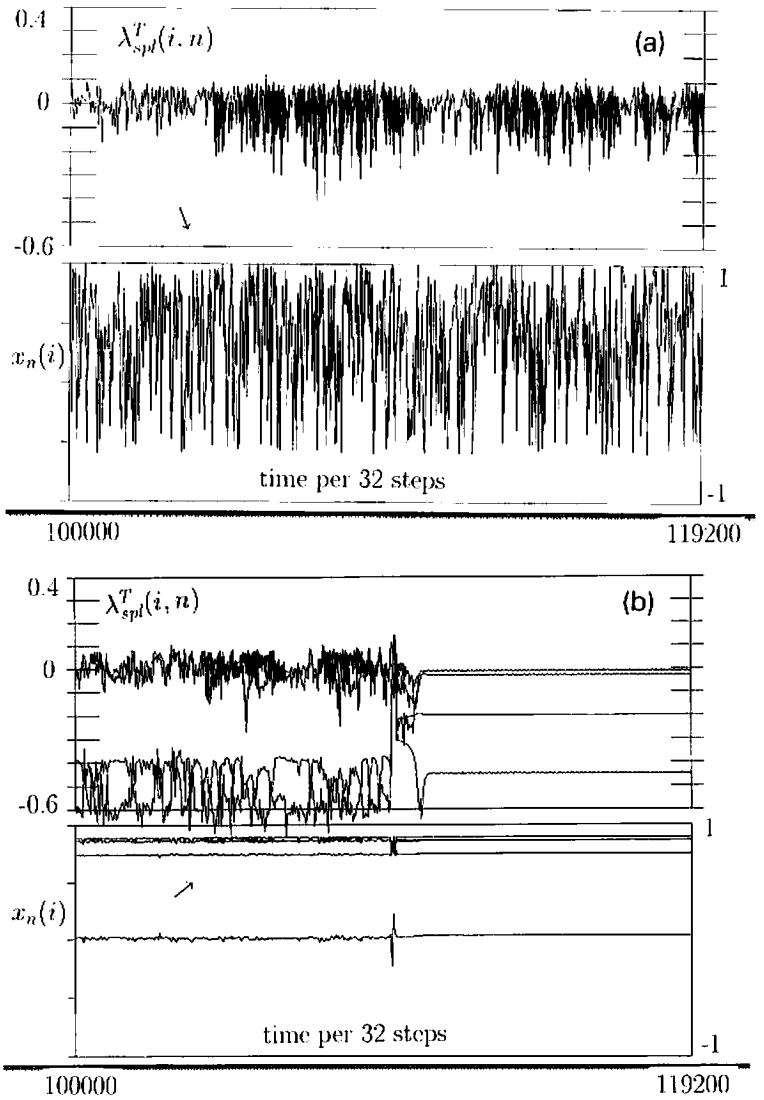

Fig. 1. Overlaid time series of $x_n(i)$ with the corresponding $\lambda^T_{\rm spl}(i,n)$. Up to the time steps indicated by the arrow, the simulation is carried out without a noise term, while the noise term with $\sigma = 10^{-8}$ is introduced later. Plotted per 32 time steps, which are chosen as the averaging time of $\lambda^T_{\rm spl}(i,n)$ (i.e., $T = 32$).

(a) $a = 1.59$,$\epsilon = 0.3$, and $N = 100$. The system had fallen on a "pseudo-attractor" with two clusters ($N_1 = 69$ and $N_2 = 31$), before the noise was added.

(b) $a = 1.90$,$\epsilon = 0.2$, and $N = 50$. The system had fallen on a "pseudo-attractor" with 4 clusters ($N_1 = 21, N_2 = 16, N_3 = 7, N_4 = 6$), and switched to a real attractor with ($N_1 = 21, N_2 = 18, N_3 = 8, N_4 = 3$) later.

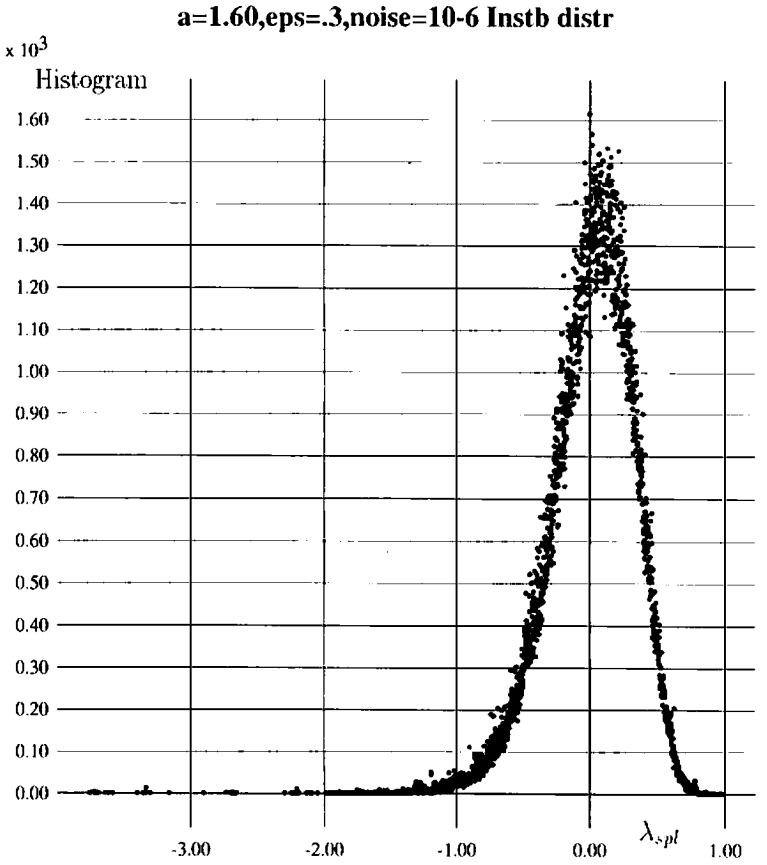

Fig. 2. Distribution of $\lambda_{spl}(i)$ for the model (2) with $a = 1.60$, $\epsilon = 0.3$, and $\delta = 10^{-6}$. The exponents are measured from the average over 128 time steps. The histogram is obtained by sampling over all elements ($N = 100$), and over 10^5 times the above 128 steps (totally 128×10^5 steps are iterated after the transient of 10^5 steps).

the splitting exponent remains close to zero, in the (type-II) PO phase around $1.57 < a < 1.61$, and $\epsilon \approx 0.3$ [1]. Thus the marginal stability is sustained not at a critical point, but over a wide range of the parameter.

3. Information cascade

It is interesting to view our dynamics as a cascade process of clustering. As is studied in [4], an attractor in the partially ordered phase can be described by successive splitting into smaller clusters. A precision-dependent cluster is defined by introducing a condition for clustering only within a certain precision. For this definition, a coarse-grained measurement is introduced as

$$\overline{x}_n^P(i) \equiv [P \times x_n(i)]/P, \tag{6}$$

[1] In the figure, drops are detected for some parameters. We note that the coherent attractor is stable if $\lambda + \log(1-\epsilon) < 0$ is satisfied, where λ is the Lyapunov exponent for a single logistic map. Due to window structures of the logistic map, λ has many drops when plotted versus a. Hence there must be some (exceptional) parameters in which the above condition is satisfied (e.g., where a logistic map shows a stable cycle). Thus $\lambda_{spl} < 0$ holds for some parameters.

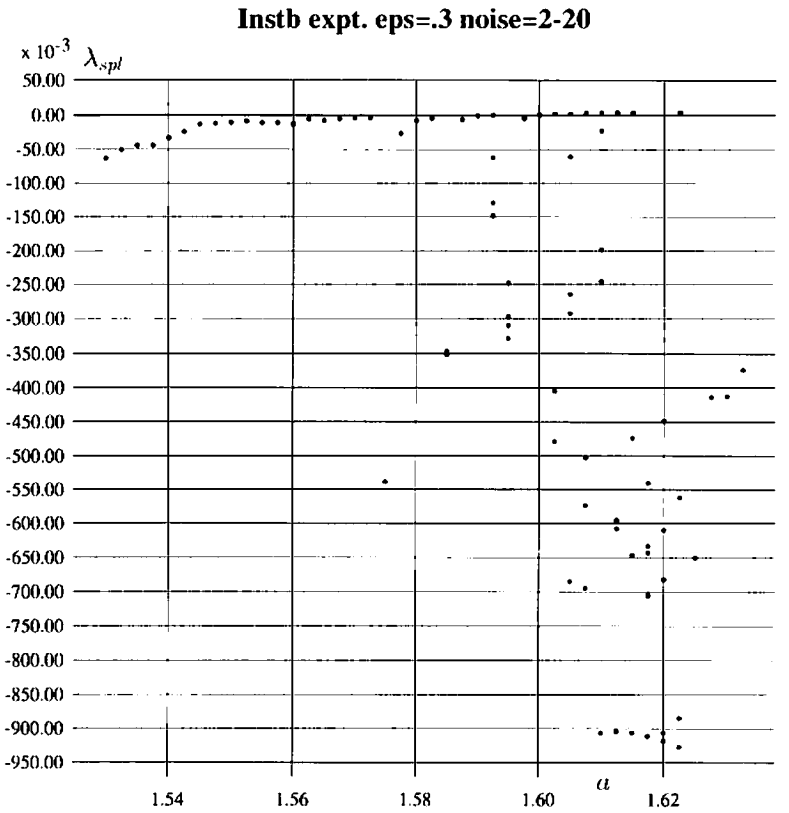

Fig. 3. The average $\lambda_{spl}(i)$ is plotted with the change of a, with $\delta = 2^{-20}$, and $\epsilon = 0.3$. The average is calculated over all elements and over 10^6 time steps. To see coexistence of attractors, 5 runs from different initial conditions are carried out for $1.59 < a < 1.62$.

where $[\cdots]$ is the integer part of $\cdots$ and P is an integer which gives the precision. By the above coarse-graining, $\overline{x}_n^P(i)$ takes only a discrete set of values with $m/P (m = 0, \pm 1, \pm 2, \ldots)$. The precision-dependent clustering is defined by the clustering for $\overline{x}_n^P(i)$. If $\overline{x}_n^P(i) = \overline{x}_n^P(j)$ holds, the elements i and j are regarded as belonging to the same cluster within that precision $1/P$. As the precision is increased, clusters split into smaller ones successively. With a given precision, a state is characterized by the number of clusters k^P and the number of elements in each cluster $[N_1^P, N_2^P, \ldots, N_{k^P}^P]$. It should be noted that the precision-dependent clustering can change in time, in contrast with the clustering of an attractor, defined through the infinite precision.

To see the partition variety of clusters, we have used the quantity defined by $Y = \sum_{j=1}^{k} (N_j/N)^2$, studied in [6,12]. Given an attractor, Y represents the probability that two arbitrarily chosen elements are in the same cluster. Instead of defining Y with infinite precision, we can straightforwardly extend the definition to finite precision, by replacing N_j and k with the corresponding quantities k^P and N_j^P with the precision $1/P$. $Y(P)$, thus defined, gives the probability that two elements i and j are in the same cluster with the precision $1/P$. In other words, $Y(P)$ is the probability that the distance between two elements i and j is smaller than $1/P$.

The partition variety $Y(P)$ is shown in Fig. 4. Y decreases with the increase of P. This decrease is due to the splitting of clusters at the precision $1/P$. We note that the decrease of Y extends down

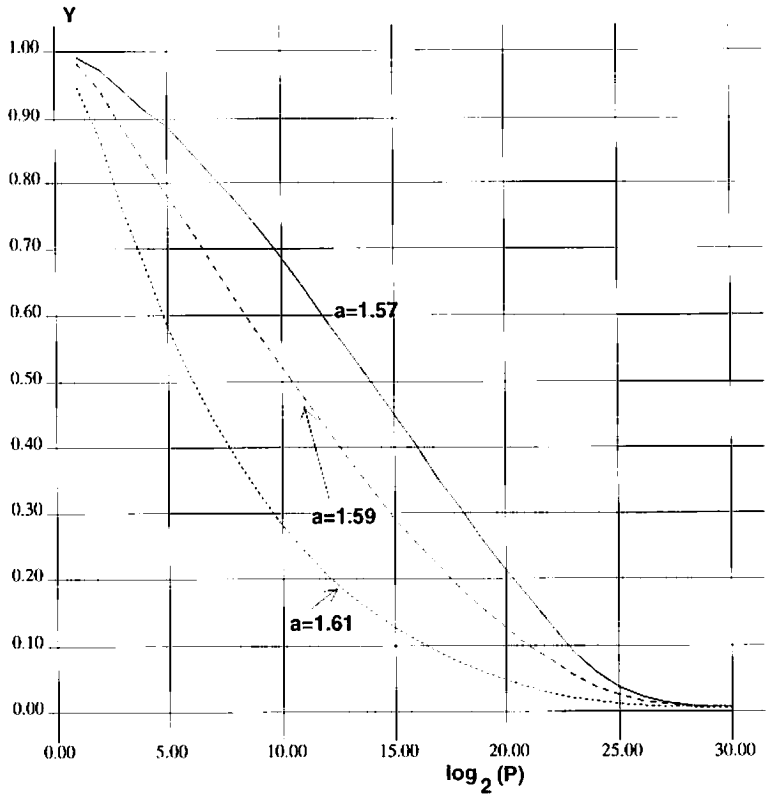

Fig. 4. Partition complexity $Y(P)$ with the precision $1/P$. P is increased as 2^j $(j = 0, 1, \ldots, 30)$. $N = 200$, $\epsilon = 0.3$, and $\delta = 10^{-8}$, for $a = 1.57, 1.59$, and 1.61. The computation is carried out for 10^5 time steps, after discarding the initial 10^4 steps.

to small P. The clustering dynamics extends to all scales here. This form is in strong contrast with that for an attractor with few clusters under the influence of noise, where $Y(P)$ has a plateau over a wide range of precisions, up to very close to the scale of the inverse of noise. The decrease of Y over a wide range of scales implies that clusters split in a cascade over a global scale.

This splitting of clusters is analogous with the cascade process of infinitely many vortices in fluid turbulence. A large vortex splits into smaller vortices, which again feed much smaller ones, and so forth [9,10]. At some time steps, a large vortex is formed with ordered motion, leading to a "coherent structure" where the motion is described by few degrees of freedom up to some precision. If we replace the term "vortex" by "cluster", this process in fluid turbulence is exactly what occurs in our system. We also note that the dynamics of vortices has a long-range interaction, while ours is global. The correspondence between our dynamics and fluid turbulence is summarized in Table 1.

In fluid turbulence, the above picture of a cascade of vortices is well established. Is it possible to detect the cascade process visually in our problem, then? To see the cascade process of clustering, we use the precision-dependent clustering to define the information flow in bit space. First, we define the entropy measuring the variety of partitioning elements into clusters as

Table 1
Correspondence between fluid turbulence and GCM

	Fluid turbulence	GCM
unit	vortex	cluster
interaction	long-ranged	global
ordering	attractive force between vortices	mean-field coupling
separation	chaotic advection field	chaos in each element
cascade	splitting into small vortices	splitting into small clusters
spatial power spectra	Kolmogorov's law	Anomalous behavior of $P(K)$
Lyapunov spectra	A[a]	A[a]

[a] Accumulation at null exponents.

$$S_n(P) = -\sum_{i=1}^{k^P} (N_i^P/N) \ln(N_i^P/N), \tag{7}$$

at a given precision $1/P$ and at time n. With the increase of P, $S(P)$ increases. The increase from $S(P = 2^j)$ to $S(P = 2^{j+1})$ gives the growth of partition information from the jth bit to the $(j + 1)$th bit. Thus we define the partition information creation (PIC) at the jth bit, by

$$I_n^j = S_n(P = 2^{j+1}) - S_n(P = 2^j). \tag{8}$$

This partition information creation tells us how much the partition variety increases at each bit. If a splitting process occurs at a bit j, the partition entropy S increases at that bit. Here, as a direct extension of the condition probability, it may be useful to introduce the conditional cluster $N_{i,i_m}^{j+1,j}$, the splitting rate of each cluster N_i when the precision is increased from $1/P = 2^{-j}$ to $1/P = 2^{-(j+1)}$, where i_m indicates a "sub"-cluster generated from the ith cluster with the above increase of the precision. Thus the PIC can be written as

$$I_n^j = -\sum_{\ell=1}^{k^{P+1}} (N_\ell^{P+1}/N) \ln(N_{i,i_m}^{j+1,j}/N_i), \tag{9}$$

where the summation over ℓ is equivalent with that over i and i_m, (i.e., $\sum_\ell = \sum_{i=1}^{k^P} \sum_{i_m}$) [2]. Thus the PIC gives the mutual information between the clusterings at the jth and $(j + 1)$th levels.

It is also possible to introduce the flow of the partition information, for example, by

$$F_n^j = S_{n+k}(P = 2^{j+1}) - S_n(P = 2^j) \tag{10}$$

which gives how the partition variety is increased to a lower bit[3] over k time steps.

In Fig. 5, the PIC is displayed in bit and time space, together with the flow of information creation. (Since the behavior of the flow F_n^j is essentially the same as the PIC I_n^j, the diagram of F_n^j is omitted later.) Over long periods of time, no creation occurs up to 30th bit, implying that the elements are coherent down to a scale of 2^{-30}. After such a quiescent region, a small difference is amplified to a larger scale, as can be seen in successive plots of the PIC. If one waits

[2] Note that the summation $\sum_{i_m}$ runs over the number of split "sub"-clusters with the increase of the precision from 2^{-j} to $2^{-(j+1)}$. If no splitting occurs it is not necessary.

[3] Here a lower bit means one that corresponds to a smaller value of 2^{-j} (i.e., larger j).

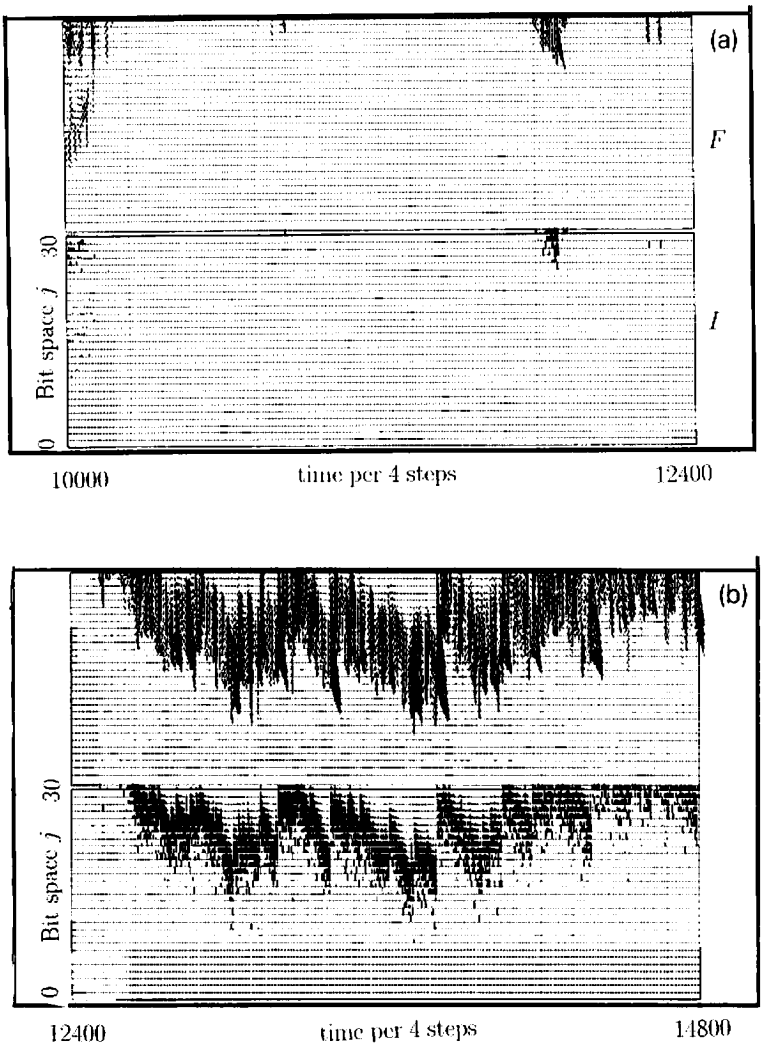

Fig. 5. Diagram of the PIC: The PIC is displayed as a diagram in bit space and time. At each pixel of the corresponding bit (j) and time (n), a box is painted whose length is proportional to I_n^j. (A scale is chosen so that the maximal size up to the next pixel gives $I_n^j = 1$). $a = 1.59$, $\epsilon = 0.3$, $N = 100$, and $\delta = 2^{-50}$. Plotted per 4 steps, over 10000–12400 (a), 12400–14800 (b), 14800–17200 (c), and 17200–19600 (d) time steps. For reference, F_n^j, the flow of the PIC is shown as the upper row of (a),(b), where the length of the arrows indicate the magnitude of the flows. (Their signs are indicated by the directions of arrows, although indiscernible in the figure.)

longer, the system comes back to the almost coherent state again. The dynamics here can be seen as an information cascade (i.e., avalanche). Successive amplification of small differences can be seen in the propagation to higher bits (smaller j). The propagation roughly has a constant speed, meaning the exponential amplification of differences. Indeed, the splitting exponent is positive in this temporal region. This avalanche in bit space stops at some scale. Then the propagation to smaller scales takes over, where negative splitting exponents determine the propagation speed in bit space.

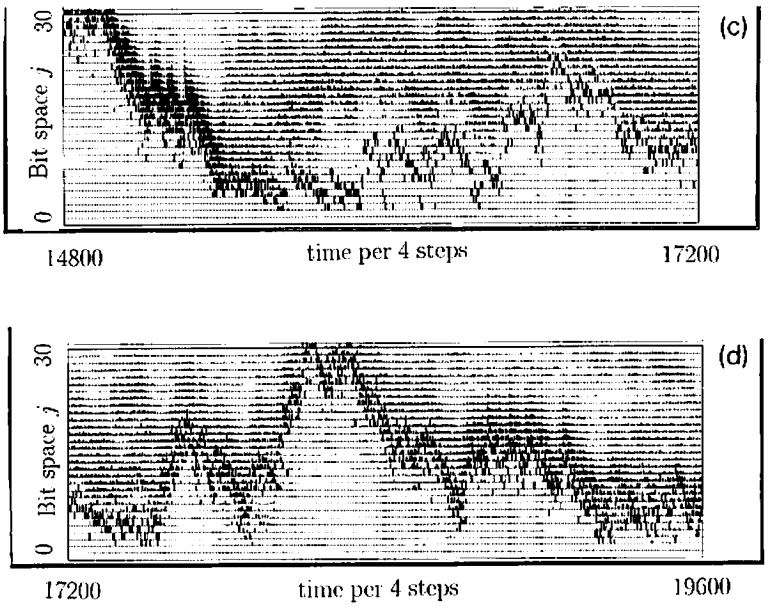

Fig. 5 (cont.).

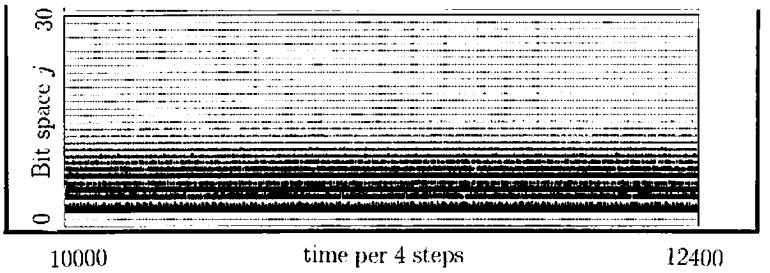

Fig. 6. Diagram of the PIC: The PIC is displayed in the same way as in Fig. 5. $a = 1.70$, $\epsilon = 0.1$, $N = 100$, and $\delta = 2^{-30}$. Plotted per 4 steps, over 10000–12400 steps.

As can be seen in the figure, the PIC flows intermittently to higher and lower bits, in the partially ordered phase. Long-term persistent propagation of the PIC is observed, leading to large fluctuations of the partition variety Y. The PIC is localized in bit space. We also note that two PIC avalanches can coexist in bit space (see Fig. 5c). In the ordered state, with small numbers of clusters, no propagation of the PIC to higher bits is observed even when some noise is introduced. In the turbulent state, on the other hand, we have observed a weak stationary PIC, localized at a low bit (see Fig. 6). The fluctuation of PIC is very small there.

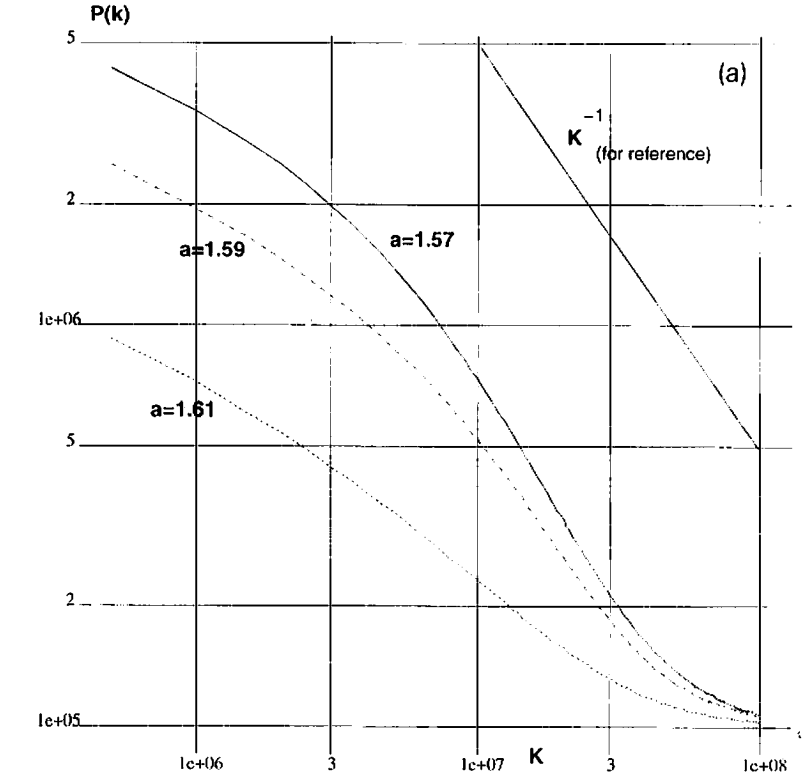
P(k)
5
2
1e+06
5
2
1e+05
(a)
K^-1
(for reference)
a=1.59
a=1.57
a=1.61
1e+06
3
1e+07
K
3
1e+08

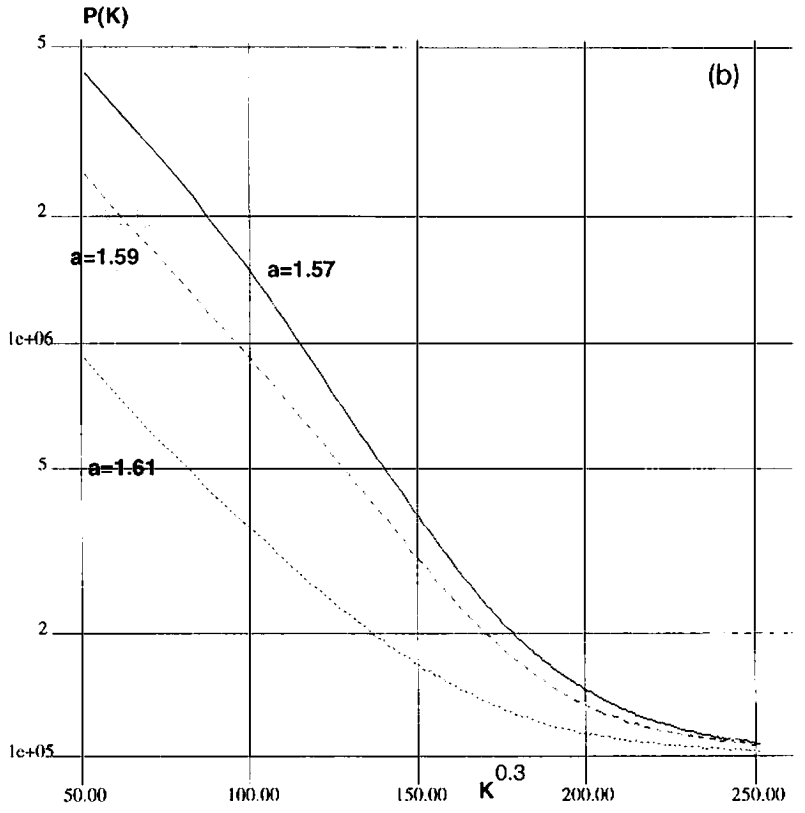
P(K)
5
2
1e+06
5
2
1e+05
(b)
a=1.59
a=1.57
a=1.61
50.00
100.00
150.00
K^0.3
200.00
250.00

Fig. 7.

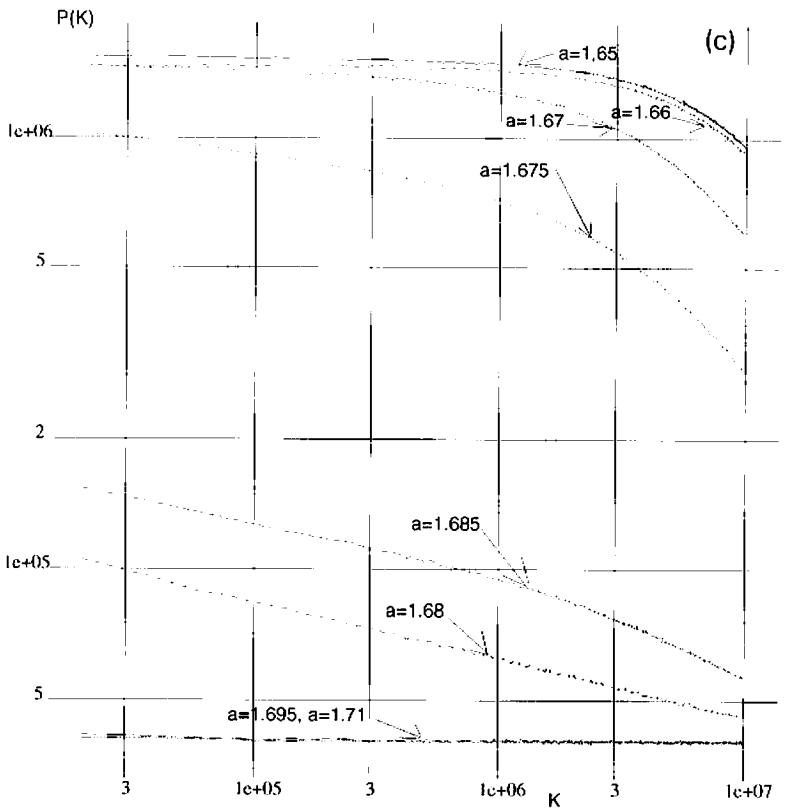

Fig. 7. Power spectra $P(K)$ for the model (2) with $N = 200$, and $\delta = 10^{-8}$. Average over the iterations of 10^5 steps, after discarding the initial 10^4 steps. (a),(b) $\epsilon = 0.3$, corresponding to the simulations of Fig. 4. (a) log–log plot (b) semi-log plot of $P(K)$ versus $K^{0.3}$. (c) $\epsilon = 0.1$, where the (type I) PO phase exists around $1.67 < a < 1.69$.

4. Power spectra and Lyapunov spectra

In turbulence in fluid dynamics, the cascade process leads to the celebrated theory of the power law of energy spectra by Kolmogorov [9,10], where the energy at the wavenumber K decreases with $K^{-5/3}$.

Since no conserved quantifiers like energy are known to exist in our system, it is not possible to straightforwardly extend our analogy to the power spectra. (Indeed the absence of an "energy" is one of the reasons why we have to introduce the PIC in the preceding section). Here we define the power spectra using the Fourier transform:

$$P(K) = \left\langle \frac{1}{N} \left| \sum_j \exp(2\pi i K x_n(j)) \right|^2 \right\rangle, \tag{11}$$

where the bracket $\langle \cdots \rangle$ denotes the temporal average. If all the elements are completely synchronized, $P(K) = N$ for any K. If the elements take random values without any correlation, $P(K)$ stays at $O(1/N)$. When there is a cascade to smaller clusters, $P(K)$ decays with K. Elements within an interval $[x, x + \Delta x]$ (i.e., in the same (precision-dependent) cluster with the precision Δx) are regarded as "synchronized" in the computation of $P(K)$ for the wavenumber $K < 1/\Delta x$. Very

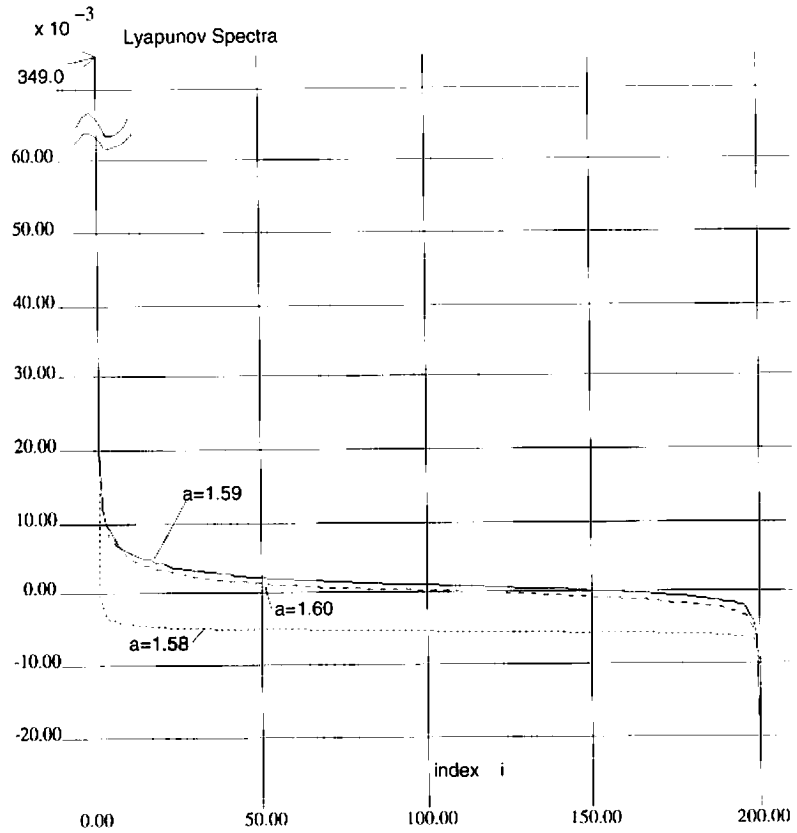

Fig. 8. Lyapunov spectra: Calculated from the product of Jacobi matrices over 2×10^4 steps, for $N = 200$, $\epsilon = 0.3$, and $\delta = 10^{-9}$. Spectra for $a = 1.58$, 1.59, and 1.60 are overlaid. For $a = 1.58$, the system falls onto a coherent cluster state ($k = 1$), which is a stable attractor. Here the first Lyapunov exponent is positive (0.349) while all others are negative (-0.04). For $a = 1.59$ and 1.6, the maximal exponent is again close to 0.349, while the second largest is approximately 0.02.

roughly speaking, $P(K)$ is approximated by $(1/N)\sum_{j=1}^{k^K}(N_j^K)^2 = NY(K)$ (for this approximation, we need to assume that the phase relationships between elements in different precision-dependent clusters are completely random). Thus a decrease of $P(K)$ implies successive splitting into smaller clusters, as is already demonstrated by the calculation of $Y(K)$. Thus the cascade process of clusters is expected to be reflected in $P(K)$.

We have plotted $P(K)$ for some parameters in the partially ordered phase (see Fig. 7). The behavior of $P(K)$ seems to be rather close to the power law form $K^{-\alpha}$ ($\alpha < 1$), but may better be fitted by a stretched exponential form $\exp(-K^{\beta})$ ($\beta \approx 0.3$) (see Fig. 7b). Although the distinction between the two forms is not easy, nevertheless, we have confirmed some anomalous behavior related with the cascade process. The behavior of $P(K)$ here is in contrast with that for the ordered and turbulent states. In the former case, $P(K)$ has a high plateau up to some value ($a \leq 1.67$ in Fig. 7c), while, at the turbulent state, $P(K)$ fluctuates around a very small value, without a significant dependence on K (see the spectra for $a \geq 1.695$ in Fig. 7c). We also note that the

power-law type behavior is more prominent near the border between the ordered and (type-II) PO phases.

Another remarkable correspondence with fluid turbulence is discernible by Lyapunov spectra, which give how a small disturbance is amplified or reduced. They are computed as the averaged logarithms of the eigenvalues of a long-time product of Jacobi matrices $J_n(i,j) = (1-\epsilon)f'(x_n(i))\delta_{i,j} + (\epsilon/N)f'(x_n(j))$. In Fig. 8, Lyapunov spectra are plotted. (For reference, the spectrum of the stable coherent state at nearby parameters is also plotted, which has one positive and $(N-1)$-fold degenerate negative exponents [4].) For the (type-II) partially ordered phase ($a = 1.59, 1.61$), we note that many exponents are accumulated around $\lambda = 0$, while few distinct positive exponents also exist. Such accumulation at the null exponent is also found in the shell model for fluid turbulence [13]. Our form of the spectra may suggest that (i) chaos is created by very few degrees of freedom, (ii) the chaotic instability is transferred to other modes, and (iii) this transfer is marginal. This picture seems to be consistent with the bit avalanche in the previous section.

5. Transition to the turbulent phase

So far we have studied the type-II partially ordered phase lying between the coherent and ordered ones. We have found that marginal stability is sustained over an interval in parameter space.

In the (type-I) partially ordered phase (between the ordered and turbulent ones), the splitting exponent λ_{spl} gradually increases from negative to positive values. Although the value is rather close to zero in the partially ordered phase, it does not stay in the vicinity of zero, but increases with the bifurcation parameter a (see Fig. 9). The marginal stability holds only at the critical point (or in a very narrow regime), in contrast with the wide parameter region for type-II.

Near the critical point, we have again observed the same behaviors as in the previous sections. We have confirmed the following properties: (1) Information cascade process with global flows to lower and higher bits as in Section 3, which is detected in a diagram of the PIC, similar to Fig. 5. (2) Power-law type behavior of the power spectra $P(K)$ (see those for $a = 1.68$ and 1.685 in Fig. 7c), similarly with the type-II case in Section 4.

It is also interesting to note the transient behavior here. Before falling onto an attractor with a small number of attractors, the system often fluctuates around a state with marginal stability. In Fig. 10, we have plotted the average of splitting exponents (over all elements and over 16 time steps). The residence near the null value is seen, where the PIC shows a behavior analogous with that in Fig. 5. Corresponding plots of the number of precision-dependent clusters are given in Fig. 10b). We note that they stay at small values over long periods of time (around 300 x 16 steps), during which the splitting exponent stays at a negative value. Here the system stays in an ordered state with a small number of clusters. The system can make itinerances over such ordered states, before falling on the attractor finally. Hence the system exhibits chaotic itinerancy over attractor ruins [4,11,8] as a transient. It is interesting to note that the high-dimensional state between two residences at ordered states satisfies marginal stability as for the separation of elements.

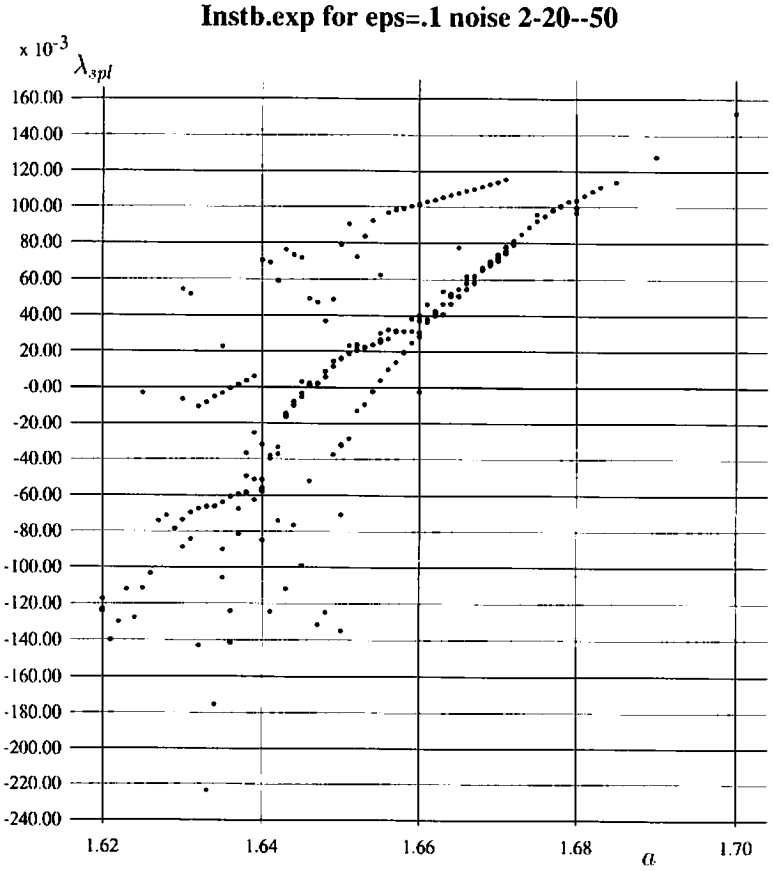

Fig. 9. The average $\lambda_{\rm spl}(i)$ is plotted versus a, with $\delta = 2^{-20}$, and $\epsilon = 0.1$. The average is calculated over all elements and over 10^6 time steps. To see the coexistence of attractors, 3 runs from different initial conditions are carried out.

6. Summary and discussion

In the present paper we have studied the cascade process of clusters in the partially ordered phases. The balance between coherence and desynchronization is demonstrated by marginal stability. In particular, the marginal stability is seen over a wide parameter region in the type-II partially ordered phase (between the ordered and coherent phases). Its mechanism is seen in the avalanche of partition information creation (PIC) in bit space.

The PIC is represented as the mutual information of partitions between a given bit and its next neighbor (see Eq. (9)). The flow of mutual information in bit space is intermittent here. Similar intermittent flow of mutual information was also noted by Matsumoto and Tsuda for a class of one-dimensional maps [14]. In contrast with the studies in low-dimensional chaos, the information

Fig. 10. Time series of $\lambda_{\rm spl}^T$ and the number of precision dependent clusters: $a = 1.93$, $\epsilon = 0.2$, $\delta = 2^{-20}$,and $N = 1000$. After around 850×16 steps the system falls on an attractor with few clusters. (a) $\lambda_{\rm spl}^T$ with $T = 16$. (b) The number of precision-dependent clusters k^P with $P = 2^8$, 2^{11}, 2^{14}, and 2^{17} from bottom to top (corresponding to (a)).

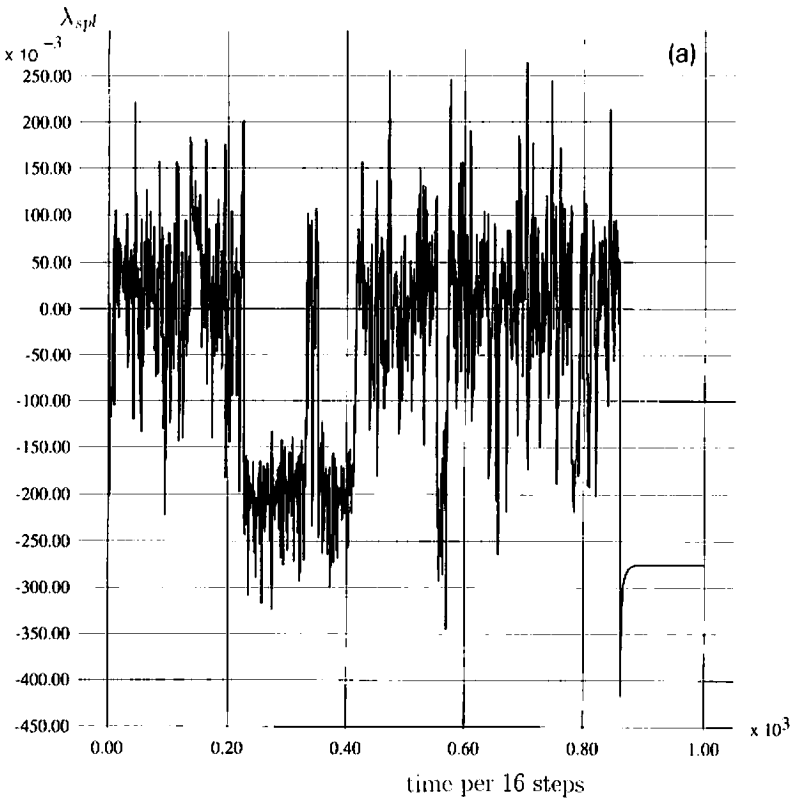
noisy gcm 2-20; a=1.93 eps=.2 N=1000 per 16 Instb
λ_{spl}
x 10^{-3}
(a)
250.00
200.00
150.00
100.00
50.00
0.00
-50.00
-100.00
-150.00
-200.00
-250.00
-300.00
-350.00
-400.00
-450.00
0.00
0.20
0.40
0.60
0.80
1.00
x 10^3
time per 16 steps

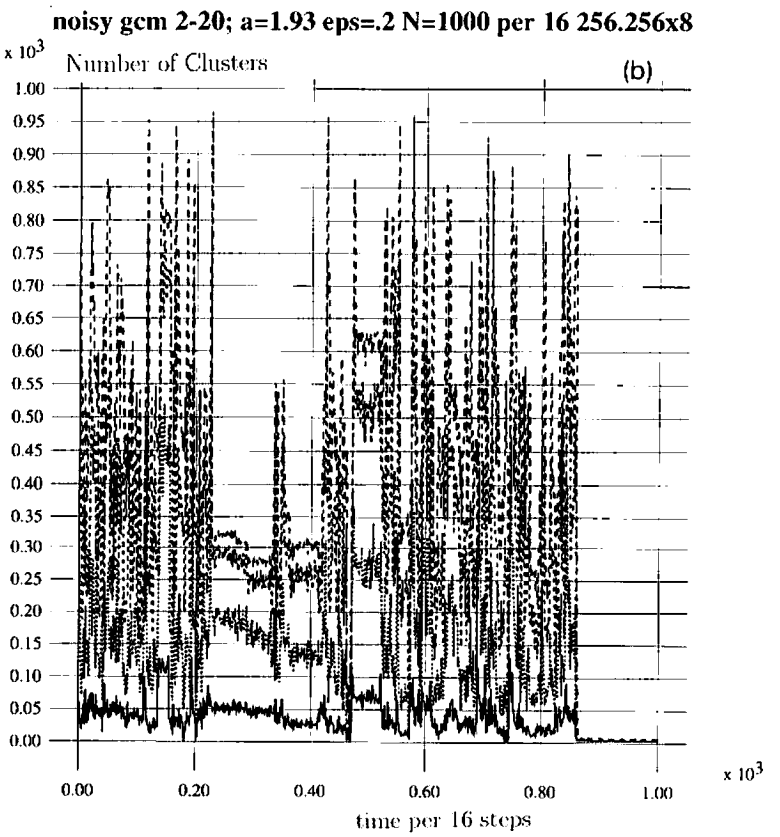
noisy gcm 2-20; a=1.93 eps=.2 N=1000 per 16 256.256x8
x 10^3
Number of Clusters
(b)
1.00
0.95
0.90
0.85
0.80
0.75
0.70
0.65
0.60
0.55
0.50
0.45
0.40
0.35
0.30
0.25
0.20
0.15
0.10
0.05
0.00
0.00
0.20
0.40
0.60
0.80
1.00
x 10^3
time per 16 steps

Fig. 10.

here measures a relation between elements rather than between two time steps.

The avalanche of the PIC demonstrates a cascade process of clusters. In analogy with the cascade process of fluid turbulence, power-law-like behavior of power spectra and accumulation of Lyapunov exponents at the null value are found. Conversely, it will also be interesting to study the cascade process of fluid turbulence in terms of the mutual information of vortices (instead of clusters here), along the line presented here.

It may be useful to mention the possible relevance of the cascade process of clusters to biological networks [17]. Dynamical change of synchronization is recently noted as a new mechanism of information processing [16,15]. In this context the importance of chaotic itinerancy [8] and marginal stability ("edge of chaos") is often discussed. The cascade process of clusters will be useful in the study of the dynamics of recall and association, and binding of relationships.

Acknowledgements

I am grateful to M. Yamada, K. Tokita, and K. Nemoto for stimulating discussions, and to F. Willeboordse for illuminating comments and critical reading of the manuscript. This work is partially supported by a Grant-in-Aid for Scientific Research from the Ministry of Education, Science, and Culture of Japan.

This paper is dedicated to Professor Kyozi Kawasaki on the occasion of his retirement from Kyushu University. About ten years ago he stressed the analogy between the pattern formation and cascade process of fluid turbulence [18]. I hope that the present paper provides another related analogy for the cascade process.

[1] K. Kaneko, Phys. Rev. Lett. 63 (1989) 219.
[2] P.Hadley and K. Wiesenfeld, Phys. Rev. Lett. 62 (1989) 1335.
[3] P. Alstrom and R.K. Ritala, Phys. Rev. A 35 (1987) 300.
[4] K. Kaneko, Physica D 41 (1990) 38; 54 (1991) 5.
[5] K. Kaneko, Phys. Rev. Lett. 65 (1990) 1391; Physica D 55 (1992) 368.
[6] K. Kaneko, J. Phys. A 24 (1991) 2107–2119.
[7] N. Nakagawa and Y. Kuramoto, Prog. Theor. Phys. 89 (1993) 313; Physica D 75 (1994) 74;
V. Hakim and W.J. Rappel, Phys. Rev. A 46 (1992) R 7347.
[8] I. Tsuda, Chaotic neural networks and thesaurus, in: Neurocomputers and Attention, eds. A.V. Holden and V.I. Kryukov (Manchester Univ. Press, 1990).
[9] A.N. Kolmogorov, C.R. Acad. Sci. USSR 30 (1941) 301, 538.
[10] See also B.B. Mandelbrodt, J. Fluid Mech. 62 (1974) 331;
U. Frisch, P.L. Sulem and M. Nelkin, J. Fluid Mech. 87 (1978) 719.
[11] K. Ikeda, K. Matsumoto and K. Ohtsuka, Prog. Theor. Phys. Suppl. 99 (1989) 295.
[12] See also M. Mezard, G. Parisi, N. Sourlas, G. Toulouse and M.A. Virasoro, J. Phys. (Paris) 45 (1984) 843;
B. Derrida, in: Nonlinear Evolution and Chaotic Phenomena, eds. G. Galavotti and P.F. Zweifel (Plenum, 1988).
[13] M. Yamada and K. Ohkitani, Phys. Rev. Lett. 60 (1988) 983;
see also K. Ikeda and K. Matsumoto J. Stat. Phys. 44 (1986) 955 for a similar behavior of Lyapunov exponents for a delayed differential equation.
[14] K. Matsumoto and I. Tsuda, J. Phys. A 21 (1988) 1405;
see also R. Shaw, Z. fur Naturforschung A 36 (1983) 80.
[15] J. Kruger, eds., Neuronal Cooperativity (Springer, New York, 1991).
[16] A. Aertsen and E.Vaadia, Coding and computation in the cortex: single-neuron activity and cooperative phenomena, in: Information Processing in the Cortex: Experiments and Theory, eds. A. Aertsen and V. Braitenberg (Springer, 1992).
[17] K. Kaneko, Relevance of Dynamic Clustering to Biological Networks, Physica D 75 (1994) 55.
[18] K.Kawasaki, talk at Conf. on Nonlinear–Nonequilibrium Statistical Mechanics (1984).